

# 顶板焊接顺序优化减小焊接变形的预测

周广涛<sup>1,2</sup>, 刘雪松<sup>2</sup>, 闫德俊<sup>2</sup>, 方洪渊<sup>2</sup>

(1. 华侨大学 机电及自动化学院, 厦门 361021;

2. 哈尔滨工业大学 现代焊接生产技术国家重点实验室, 哈尔滨 150001)



周广涛

**摘 要:** 利用热弹性有限元方法对材料 Q345 大型吊车箱形梁分段的顶板结构焊接变形进行了数值模拟计算, 建立了分析模型, 定量地描述了纵筋与顶板焊接顺序及横筋与顶板焊接顺序对焊接变形的影响, 并按照“与”的关系结合两者的最优化焊接顺序形成整体焊接结构的最佳焊接顺序. 对预测的最佳焊接顺序下的变形模拟值和测量值进行了对比. 结果表明, 两者吻合良好, 最优与最差的焊接顺序得到的变形量为 15.12 和 28.47 mm, 降低了 47%, 为实际生产提供了可靠的数值预测依据.

**关键词:** 数值模拟; 焊接顺序; 优化; 预测

**中图分类号:** TG115.28    **文献标识码:** A    **文章编号:** 0253-360X(2009)09-0109-04

## 0 序 言

焊接变形影响焊接结构尺寸的精度, 使结构之间装配困难, 或者勉强装配后, 产生超过容许限度的装配应力而减弱承受能力. 焊接顺序对残余应力和变形产生的影响极大, 因此质量要求较高的焊接结构均要在其焊接工艺流程中安排合理的焊接顺序<sup>[1]</sup>.

实际生产中对于焊接变形的控制主要依靠经验和大量的试验, 在产品出现焊接变形超出设计尺寸要求时还须采取其它矫正措施, 这样做既增加了成本, 又会改变残余应力的分布状态<sup>[2]</sup>. 优化焊接顺序来控制焊接变形相对于其它方法是最简单易行又节约成本的. 随着计算机的发展, 有限元数值模拟计算方法可以避免以往单纯依靠经验、耗费成本的试验来摸索参数的缺点<sup>[3-7]</sup>.

文中以吊车某一箱形梁组段的顶板焊接结构为研究对象, 箱形梁焊接生产过程中最突出的问题就是存在较大焊接变形, 因此研究上盖板的焊接过程, 找到减小其焊接残余变形量的方法, 对于实际生产具有十分重要的意义.

文中应用 Marc 软件对顶板结构的焊接变形进行了数值模拟计算, 计算结果对优化焊接顺序、减小焊接变形提供了有价值的理论预测, 为实际焊接生产提供合理的组合方案.

## 1 顶板模型建立

### 1.1 顶板模型与有限元模型建立

顶板结构由顶板、2 条 T 形纵筋和 4 条横筋焊接组合而成, 如图 1 所示. 该结构尺寸大, 底板尺寸为 13.6 m×4.11 m×0.032 m; 纵筋尺寸为 13.6 m×0.25 m×0.01 m; 横筋尺寸为 2.905 m×1.015 m×0.01 m. 接头均为 T 形, 角焊缝布置在筋板两侧. 以每独立筋板按照 2 条焊缝计, 焊缝共有 12 条.

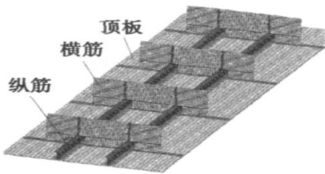


图 1 有限元模型网格划分  
Fig. 1 Mesh of FEM model

将模型建成三维实体模型, 由于模型尺寸大, 按照常规离散有限元模型将会使网格划分数量巨增, 数目巨大的网格由于计算机 CPU 的容量限制和本身庞大的计算量会造成计算的无法进行, 或者计算时间大大加长. 为了缩短计算量, 保证计算进行顺利, 提高计算效率并保证计算精度, 采取一些措施对模型进行简化. 采用较粗大的网格尺寸, 模型单元为八节点六面体类型, 最大边长可达 40 mm, 在温度

梯度变化大的焊缝及其附近区域网格加密处理, 在离焊缝较远处和温度变化不明显的区域, 采用较稀疏的网格, 整体上表现为由密到疏的过渡方式. 模型如图 1 所示, 共含 66 384 个单元、126 714 个节点.

表 1 Q345 材料热物理及力学性能

Table 1 Thermo-mechanics characteristic for Q345

温度 $T/^{\circ}\text{C}$	导热率 $\lambda/(\text{W}\cdot\text{m}^{-1}\cdot^{\circ}\text{C}^{-1})$	比热容 $c/(\text{J}\cdot\text{K}^{-1}\cdot^{\circ}\text{C}^{-1})$	线膨胀系数 $\alpha_l/(10^{-6}\cdot^{\circ}\text{C}^{-1})$	弹性模量 $E/\text{GPa}$	屈服强度 $R_{\text{el}}/\text{MPa}$
20	48	461	11.9	212	343
200	47.5	533	13	199	276
400	41.6	611	14.1	184	167
600	35.5	778	14.9	164	0.5
1 500	36	780	15	73.75	0.35

1.3 热源模型选择

焊接过程模拟计算是热-力耦合过程, 热分析模拟计算量大, 因此选择计算效率高的热源形式很必要, 文中在焊接模块里对热源尺寸进行了修订, 使得热源单位时间内覆盖的长度比常规大十倍, 原理上是分段串状热源的衍生, 该热源经过验证在大型构件的模拟计算中是可行的<sup>[8]</sup>. 这样焊接速度可达 50 mm/s, 计算速度加快.

2 不同焊接顺序下变形模拟计算结果

2.1 T 形接头两侧角焊缝焊接顺序确定

每条 T 形接头都是立筋由左右两条焊缝焊在顶板上. 对 T 形接头焊后变形的影响进行了局部焊接数值模拟, 结果表明, 如果先焊接左焊缝, 再接着焊右焊缝, 最终产生向左侧偏转, 如果左右两条焊缝同时施焊, 立筋几乎无偏转. 因此, 每个筋板的两条焊缝应该同时施焊. 以下模拟方案均是在此基础上完成, 这样焊缝的布置实际变成了 6 条. 鉴于结构焊缝数量组合顺序较多, 根据实际生产经验组合方案, 可以将纵筋与顶板的焊接和横筋与顶板的焊接分别计算优化, 进而组成整体结构的合理焊接顺序.

2.2 纵筋与顶板焊接顺序对焊接变形影响

纵筋与顶板的焊缝采取两种方案分配焊接顺序, 第一种方案是从左至右的焊接顺序; 第二种方案是从中心向两边的焊接顺序. 两种方案焊接顺序如图 3 所示. 实线箭头表示按顺序焊接, 虚线箭头表示同时焊接, 箭头的指向代表焊接的起止方向. 焊后变形模拟结果如图 3 所示. 文中主要以其变形后结构中最高点和最低点的差值为考察量, 定义为  $\Delta H$ . 各方案计算得出的  $\Delta H$ , 如表 2 所示.

由表 2 的变形计算结果可以观察到, 焊接顺序

1.2 材料特性

材料的热物理及力学参数均随温度而变化, 对于焊接模拟结果准确性有着重要的作用, 模拟采用的材料为 Q345, 各性能参数随温度变化的情况见表 1.

的改变对挠度差  $\Delta H$  影响较大, 图 2a<sub>2</sub> 的焊接顺序(先焊接①, 接着反向焊②)所得到的焊接挠度变形量最小. 按照这种焊接顺序得到的  $\Delta H=11.707$  mm, 比图 2a<sub>4</sub> 中所所示的焊缝①②反向同时焊接得到的  $\Delta H=13.465$  mm 小 1.758 mm. 图 2b<sub>2</sub> 的焊接顺序(先①②, 接着③④)所得到的焊接挠度变形量最

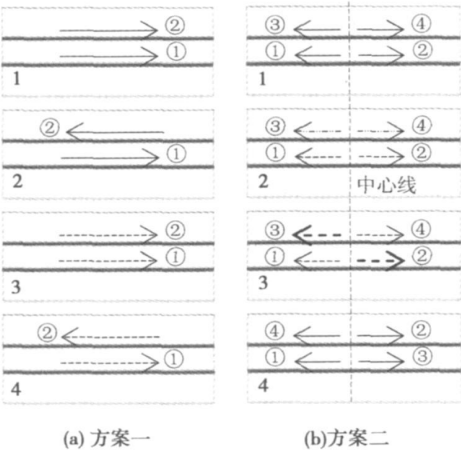


图 2 纵筋与顶板焊接顺序两种方案  
Fig 2 Welding sequences under two schemes

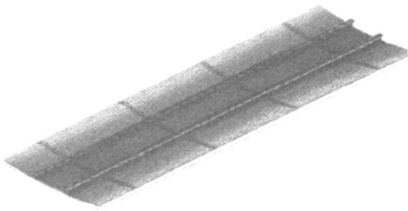


图 3 焊接变形模拟结果云图  
Fig. 3 Contour of welding deformation

表 2 纵筋与顶板焊接变形计算结果对比

Table 2 Welding deformation under different welding sequences

焊接顺序 编号	第一方案		第二方案	
	焊接顺序	挠度差 $\Delta H_1$ /mm	焊接顺序	挠度差 $\Delta H_2$ /mm
1	先①后②	13.287	①②③④ 顺次焊接	11.988
2	先①后②	11.707	①②同时 ③④同时	11.983
3	①②同时	12.912	①④同时 ②③同时	13.707
4	①②同时	13.465	①②③④ 顺次焊接	12.352

小. 按照这种焊接顺序得到的  $\Delta H=11.983\text{ mm}$ , 比图 2b<sub>3</sub> 中所示的焊缝①④接着②③同时焊接得到的  $\Delta H=13.707\text{ mm}$  小 1.724 mm. 因此, 采取每条焊缝从头到尾并如图 2a<sub>2</sub> 的顺序较为合理.

2.3 横筋与顶板焊接顺序对焊接变形影响

每条横筋由 3 段两侧对称分布的焊缝组成, 这 3 段焊缝的焊接顺序对横向的变形影响较小, 主要是引起长度方向的角变形, 因此在模拟计算时, 这 3 段焊缝作为一条整体焊缝来处理.

焊接顺序如图 4 所示. 仍用实线箭头表示按顺序焊接, 虚线箭头表示同时焊接, 箭头的指向代表焊接的起止方向. 焊后变形模拟结果如图 5 所示. 在

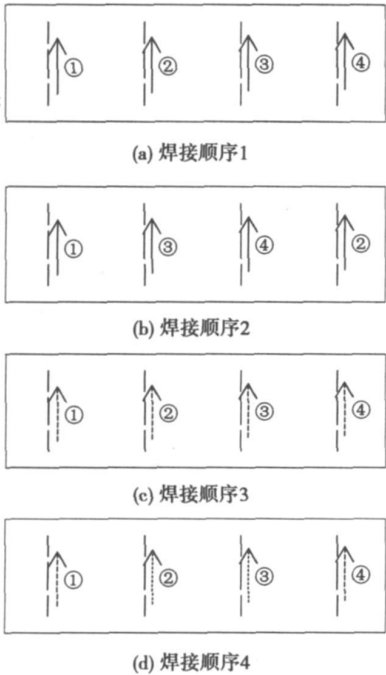


图 4 横筋与顶板焊接顺序示意图

Fig 4 Schematic plan of different welding sequences

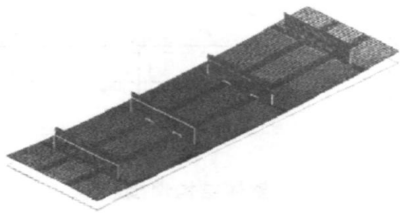


图 5 角变形模拟结果  
Fig. 5 Angular deformation

宽度方向没有明显变化, 在长度方向表现为角变形, 这是该结构最主要的变形. 总体变形是四条横筋各自引起角变形的叠加, 文中仍以其变形后结构中最高点和最低点的差值为考察量. 各方案计算得出的挠度差  $\Delta H$ , 如表 3 所示.

表 3 横筋与顶板焊接变形计算结果对比

Table 3 Welding deformation under different welding sequences

焊接顺序编号	焊接顺序	挠度差 $\Delta H$ /mm
1	①②③④顺次焊接	18.57
2	①②③④依次焊接	15.682
3	①②③④同时焊接	14.021
4	①④同时之后②③同时	12.352

模拟计算发现, 焊缝反向施焊对于角变形角度的变化几乎没有影响, 因此组合顺序可以简炼到上述 4 种. 由表 3 可以看出, 4 条焊缝①②③④同时焊接的变形量  $\Delta H_3=14.021\text{ mm}$  比 4 条焊缝依次焊接的变形量  $\Delta H_1=18.57\text{ mm}$  小了 4.449 mm, 如果焊接时角接头不受拘束, 结构将在每个接头处弯曲而形成 一个多边形, 从而使结构折弯而起, 向收缩量大的一侧弯, 这主要是沿厚度方向的横向收缩不均匀、有梯度造成的. 因此依次焊接的变形角度大, 焊缝同时焊接的变形由于热输入分散使得温度分布差异不明显, 横向收缩减小, 焊后的角度收缩也相应减小.

3 整体结构焊接变形模拟结果与测量

通过数值模拟, 得出在整体组合状态下焊接纵向筋板按照表 1 的顺序得出的规律依然正确, 只是数值比相应变形要低. 在纵向长筋板固定情况下, 焊接 4 条横筋, 变形的趋势大小与表 3 符合.

整个焊接结构的焊接顺序优化原则就是将部件焊接模拟的最佳焊接顺序组合在一起, 符合算法中”与”的关系, 既满足纵筋的最小变形顺序, 又满足横筋与板的最小变形顺序, 如图 6 所示.

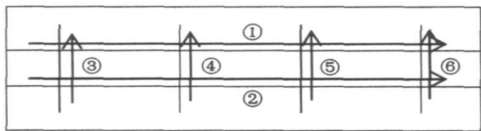


图 6 整体结构焊接顺序  
Fig. 6 Welding sequences of whole structure

焊接变形外观模拟结果如图 7 所示。对两种极端的情况进行了对比计算。(1) 图 6 中②与①(与箭头反向)同时焊接,焊完后开始进行③④⑤⑥顺次焊接;(2) 先②依次①,焊完后③⑥同时,最后⑤④同时焊接。结果表明,情况(1)变形最大,  $\Delta H$  达 28.47 mm;情况(2)变形最小,  $\Delta H$  达 15.1 mm,减小了约 47%。可见依靠优化焊接顺序可以在一定限度内减少焊接变形,但为了取得更好的效果还需要配合其它的手段,如采取预反变形装配或者加强约束等。由于筋板的交叉,实际施焊时,对于每条焊缝从头焊到尾比较容易操作,比较合理。不建议以中心向两边焊接,通过模拟,经验性的从中心向两边的焊接变形并不是最小的。

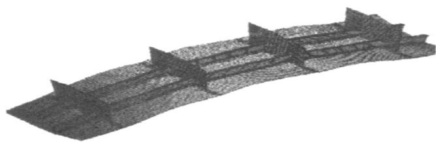


图 7 整体结构焊接变形模拟结果  
Fig. 7 Simulation result of welding deformation

对上述两种极端焊接顺序进行了实际焊接测量,实际测量值小于计算值,顺序(1)实际测量值为 22.30 mm,顺序(2)为 12.11 mm,如图 8 所示。

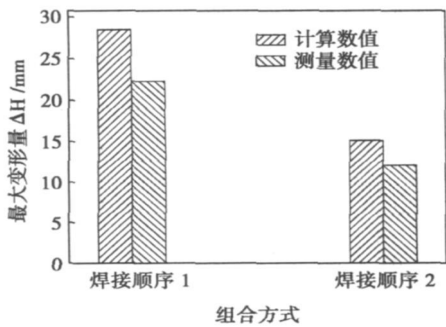


图 8 两种极端焊接顺序变形对比  
Fig. 8 Comparison of deformation under two extreme conditions

4 结 论

- (1) 对于文中结构,将纵筋与顶板的焊接顺序和横筋与顶板的焊接顺序分别计算优化,得出纵筋与顶板最佳焊接顺序是从左向右焊接第一条焊缝,再反向从右向左焊接第二条焊缝,变形可减少 13%;横筋与顶板的最佳焊接顺序是外侧两条横缝同时先焊接,中部两条焊缝再同时焊接,变形减少 33%。
- (2) 所有部件组装定位焊成一整体时,可增加结构的刚性,焊接后各种对应的变形将减小。将分别优化计算的最佳结果按“与”的算法组合在一起得到最小的焊接变形为 15.12mm,比最大的变形量 28.47 mm 降低了 47%。计算所得的焊接顺序对焊接变形的影响规律、为顶板的焊接实际生产提供了可靠的数值预测依据。

参考文献:

[ 1 ] 田锡唐. 焊接结构[ M ]. 北京: 机械工业出版社, 1982.

[ 2 ] 拉达伊 D. 焊接热效应[ M ]. 熊第京, 译. 北京: 机械工程出版社, 2004.

[ 3 ] 崔晓芳, 岳红杰, 兆文忠, 等. 高速机车构架侧梁的焊接顺序[ J ]. 焊接学报, 2006, 27(1): 101—104.

Cui Xiaofang, Yue hongjie, Zhao Wenzhong *et al.* Study of different welding sequences in the bogie frame of the high-speed locomotive[ J ]. Transaction of the China Welding Institute, 2006, 27(1): 101—104.

[ 4 ] 牛济泰. 材料和热加工领域的物理模拟技术[ M ]. 北京: 国防工业出版社, 1999.

[ 5 ] Cai Z, Zhao H, Lu A. Efficient finite element approach for modeling of actual welded structures[ J ]. Science and Technology of Welding and Joining, 2003, 8(3): 195—204.

[ 6 ] 谢智华. 钢桥主桁箱形梁焊接工艺及其变形的控制[ J ]. 焊接, 1999(9): 25—27.

Xie Zhihua. Welding procedure and distortion control for bridge box beam[ J ]. Welding & Joining, 1999(9): 25—27.

[ 7 ] Brown S, Song H. Finite element simulation of welking of large structures. journal of engineering for industry[ J ]. Transactions of ASME, 1992, 114(4): 441—451.

[ 8 ] 蔡志鹏, 赵海燕, 鹿安理, 等. 焊接数值模拟中分段移动热源模型的建立与应用[ J ]. 中国机械工程, 2002, 13(3): 208—210.

Cai Zhipeng Zhao Haiyan, Lu Anli, *et al.* Establishment of line-gauss heat source model and application in welking numerical simulation[ J ]. China Mechanical Engineering, 2002, 13(3): 208—210.

作者简介: 周广涛, 男, 1973 年出生, 博士研究生. 主要从事焊接结构力学与可靠性分析、裂纹控制和数值模拟. 发表论文 6 篇.

Email: zhougt-hit@sina.com

determined. Effect of argon arc remelting parameters on microstructure and mechanical properties of hot dipping aluminizing surface was investigated. The results show that for the hot dipping aluminizing coating after argon arc remelting treatment, stratification phenomenon disappeared, gradient transition on microstructure appeared, specimen consisted of remelting layer, transition layer and substrate. Argon arc remelting treatment can obviously increase microhardness of hot dipping aluminizing coating. The process parameters influence the depth, hardness and crack rate of the remelting layer markedly. With the welding current increasing or the welding speed decreasing, the remelting layer depth and hardness increases and the crack rate decreases.

**Key words:** hot dipping aluminizing (HDA); argon arc remelting; microstructure; microhardness

### Simulation of viscoelastic heat during ultrasonic welding of thermoplastics

ZHANG Zhenqiang<sup>1</sup>, ZHANG Zongbo<sup>1</sup>, LUO Yi<sup>1,2</sup>, WANG Xiaodong<sup>1,2</sup>, WANG Liding<sup>1,2</sup> (1. Key Laboratory for Precision and Non-traditional Machining Technology of Ministry of Education, Dalian University of Technology, Dalian 116024, Liaoning, China; 2. Key Laboratory for Micro/Nano Technology and System of Liaoning Province, Dalian 116024, Liaoning, China). p 97—100

**Abstract:** Viscoelastic heat is one of the main heat sources during ultrasonic welding of thermoplastics. Unfortunately the present works could not definitely take into account the dynamic viscoelasticity of thermoplastics. In this paper a simplified method was proposed to characterize dynamic viscoelasticity based on static relaxation modulus and TTEP (time-temperature equivalent principle). The method could represent dynamic modulus as the function of temperature and frequency, and avoids calculating dynamic modulus of high frequency by shifting and extrapolating the dynamic modulus of lower frequency from experiments. With the method mentioned above, a strategy was put forward to simulate the viscoelastic heat of PMMA (polymethylmethacrylate) under periodic load using FEM (finite element method). The calculated temperature shows a similar tendency as tested results in other literatures.

**Key words:** ultrasonic welding; dynamic viscoelasticity; viscoelastic heat; finite element method

### Joints performance of diffusion bonding between pure Cu and stainless steel and dynamic analysis of atomic diffusion

LIU Shuying (Key laboratory of Advanced Non-ferrous Metals, Henan University of Science and Technology, Luoyang 471003, Henan, China). p 101—104

**Abstract:** The effects of welding parameters on the performance of the joints of pure copper and ferrite 410L and joints of pure copper and austenite 304 stainless steel were researched by microstructure observation, hardness, tensile test and EPMA. And atomic diffusion mechanism of two kinds of joints combined theoretical calculation was also discussed. The result indicated: as bonding pressure and bonding time fixed, the joints tensile strength increased with the bonding temperature. Optimal bonding temperature of Cu/

410L is about 50 K lower than that of Cu/304, because the diffusion speed of Cu, bcc ferrite is faster than in fcc austenitic. The measured diffusion speed of Cu atom in stainless steel is smaller than the theoretical value because the theoretical value was obtained based on assuming 100% full adhesion for the surface in initial, but the actual bonding surface is rough in initial stages.

**Key words:** diffusion bonding; diffusion speed; ferritic; austenitic; tensile strength

### Microstructure and properties of 65Mn spring steel by laser welding

LIU Qibin, LI Bin (Materials School of Guizhou University, Caijiaguan Branch, Guiyang 550003, China). p 105—108

**Abstract:** To obtain excellent welding joint, 65Mn spring steel was welded by 5 kW CO<sub>2</sub> laser welding equipment. Microstructure, tensile strength, tensile fracture and residual stress of this joint were investigated by means of OM, XRD, SEM, microhardness testing machine, electronic universal testing machine and residual stress test machine. The experimental results indicate that the fine equiaxed crystal, dendrite crystal and cell grain are formed from welding central zone to edge zone, respectively. In the HAZ, the over-heated zone is mainly comprised of coarse acicular martensite. Recrystalline zone mainly consists of fine acicular martensite. The part transforming zone is comprised of ferrite and pearlite. The welding joint mainly consists of fine  $\alpha$ -Fe, Fe<sub>3</sub>C and FeSi. The highest hardness value of welding zone and HAZ is 720 HV and 770 HV, respectively. The hardness decreases significantly from HAZ to base metal. The average tensile strength of welding joints is approximately 475 MPa. The average residual stress in welding zone is 105 MPa, and the average residual stress in HAZ is -60 MPa.

**Key words:** spring steel; 65Mn; laser welding; microstructure; properties

### Prediction for welding deformation reducing by welding sequence optimization of upper plate

ZHOU Guangtao<sup>1,2</sup>, LIU Xuesong<sup>2</sup>, YAN Dejun<sup>2</sup>, FANG Hongyuan<sup>2</sup> (1. College of mechanical Engineering and Automation, Huaqiao University, Xiamen 361021, China; 2. State Key Laboratory of Advanced Welding Production Technology, Harbin Institute of Technology, Harbin 150001, China). p 109—112

**Abstract:** The numerical simulation of welding deformation of upper plate structure for large-scale crane box beam was conducted using the thermo elastic-plastic method. Analysis model was established to quantitatively describe the effects of welding sequence for both longitudinal rib to upper plate and transverse rib to upper plate on welding deformation. The optimal welding sequence of the whole structure was obtained by the term of the “and” relation. The simulation value of deformation under the optimal welding sequence was contrast to measured value to show the better agreement for two values. The deformation of the optimal sequence and the worst sequence was 15.12 mm and 28.47 mm, respectively.

**Key words:** numerical simulation; welding sequence; optimal; prediction